Site U1358[1]

Expedition 318 Scientists[2]

Chapter contents

Site summary 1
Operations 2
Lithostratigraphy 2
Biostratigraphy 3
Geochemistry 4
Physical properties 4
References 5
Figures 7
Tables 14

Site summary

Integrated Ocean Drilling Program Site U1358 (proposed Site WLSHE-08A) is on the continental shelf off the Adélie Coast (Fig. F1) at 501 meters below sea level (mbsl). The main objective at Site U1358 was to core across regional unconformity WL-U8. This unconformity marks a distinct change in the geometry of the progradational wedge from low-dipping strata below to steeply dipping foresets above (Eittreim et al., 1995; Escutia et al., 1997; De Santis et al., 2003) (Fig. F2). This is inferred to represent a significant change from intermittent glaciers to persistent oscillating ice sheets, either during the late Miocene (Escutia et al., 2005; Cooper et al., 2009) or during the late Pliocene (~3 Ma) (Rebesco et al., 2006). The steep foresets above unconformity WL-U8 are thought to likely consist of ice proximal (i.e., till, diamictite, and debris flows) and open-water sediments deposited as grounded ice sheets extended intermittently onto the outer shelf, similar to sediments recovered at Ocean Drilling Program Site 1167 on the Prydz Bay Trough fan (O'Brien, Cooper, Richter, et al., 2001; Passchier et al., 2003).

Site U1358 lies at the westernmost edge of the Mertz Bank (Fig. F1) and receives drainage from the East Antarctica Ice Sheet through the Wilkes subglacial basin (Fig. F4 in the "Expedition 318 summary" chapter). At Site U1358, unconformity WL-U8 occurs at ~165 meters below seafloor (mbsf) (0.84 s two-way traveltime) (Fig. F2). Multichannel seismic reflection profiles crossing Site U1358 show gently dipping strata on the shelf that are truncated near the seafloor (Fig. F2). This provided a unique opportunity to sample across the unconformity by drilling at very shallow penetration. The record from Site U1358 will also complement the more distal (i.e., glacial–interglacial cycles) record from Sites U1359 and U1361, located on the continental rise.

We drilled two short holes at Site U1358 in a water depth of 501 mbsl. Unfortunately, we were only able to penetrate to 35.6 mbsf before the drill collars failed and we had to abandon the hole.

Hole U1358A was drilled to a total depth of 2.0 mbsf and Hole U1358B was drilled to a total depth of 35.6 mbsf, both using the rotary core barrel (RCB) system. The upper 8.2 m is unconsolidated and moderately to strongly disturbed by drilling. Below 8.2 mbsf, the sediments are consolidated and only slightly disturbed by drilling. Holes U1358A and U1358B penetrated diamictons and diamictites and are placed within a single lithostratigraphic unit (Fig. F3). The diamictons in the upper 8.2 mbsf were probably

[1] Expedition 318 Scientists, 2011. Site U1358. *In* Escutia, C., Brinkhuis, H., Klaus, A., and the Expedition 318 Scientists, *Proc. IODP,* 318: Tokyo (Integrated Ocean Drilling Program Management International, Inc.). doi:10.2204/iodp.proc.318.106.2011
[2] Expedition 318 Scientists' addresses.

doi:10.2204/iodp.proc.318.106.2011

deposited from floating ice. The diamictites below 8.2 mbsf were either deposited from floating ice, where crudely stratified and laminated, or subglacially with possible remobilization by glacigenic debris flow.

Sediments in Holes U1358A and U1358B contain siliceous and organic microfossils. Diatom biostratigraphy provides tentative stratigraphic control throughout the section. Pliocene strata (9.32–28.62 mbsf) are overlain by uppermost Pleistocene to Holocene strata. Dinocysts and radiolarians were encountered in trace amounts only and provide no further age constraints. Foraminifers were not encountered in holes drilled at Site U1358. Diatom assemblages suggest a high-nutrient, open-water environmental setting, similar to that of the modern-day Southern Ocean north of the winter sea ice extent. Palynological associations are a mix of reworked and in situ palynomorphs. In situ protoperidinioid dinocysts confirm a nutrient-rich environment. High abundances of reworked Mesozoic/Paleozoic microfossils indicate a significant input of eroded sediments.

Whole-core magnetic susceptibility was measured at 2.5 cm intervals (2 s measurement time). The raw data values range from 3 to 2834 instrument units (Fig. F4). However, the majority of measurements vary between 200 and 400 instrument units, with some peaks in Core 318-U1358B-4R representing gravel clasts. Variations in gamma ray attenuation (GRA) density reflect variations in the composition of the Pliocene–Pleistocene diamictite that varies between clast-rich muddy and clast-rich sandy lithologies.

Operations

Transit to Site U1358

Transit from Site U1357 to Site U1358 began at 0900 h on 6 February 2010. We proceeded on an easterly course along the Wilkes Land coast and briefly into the Antarctic Circle (66°33.65′S and 140°43.70′E) before turning to the northeast toward the shelf drill sites (U1358 and U1360). As we approached Site U1360, the Captain decided from visual and radar observations that there was too much floating ice in the vicinity for safe operations. This concentration of ice would likely force us to make an early departure to avoid entrapment caused by the severe weather predicted for late 7 February. We continued past Site U1360 to Site U1358, which is closer to open waters and therefore might allow us stay on location longer before the predicted storm would arrive. The 93 nmi transit was accomplished at an average speed of 10.9 kt. All times in this section are given in local ship time, which was Universal Time Coordinated + 11 h.

Site U1358

Hole U1358A

The ship was positioned over Site U1358 at 1730 h on 6 February. The drill string was lowered to the seafloor, but we had to wait 1.3 h to start coring as an iceberg moved through the drilling area. We tagged the seafloor with the bit at 510.0 meters below rig floor and started RCB coring in Hole U1358A at 2245 h on 6 February.

While cutting Core 318-U1358A-1R, an iceberg approached close enough to the vessel that we had to pull out of the seafloor at 0015 h on 7 February. We moved 300 m south-southwest of the hole to allow the iceberg to pass. Drilling Core 318-U1358A-1R penetrated only 2.0 m and recovered 1.10 m (55%) (Table T1).

Hole U1358B

After waiting 2.25 h for the iceberg to drift out of the area, we moved back over the site and started Hole U1358B at 0250 h on 7 February. RCB Cores 318-U1358B-1R through 4R penetrated to 35.6 mbsf and recovered 8.0 m (22%) (Table T1).

While attempting to cut Core 318-U1358B-5R, a drill collar connection failed and the lower stand of drill collars, mechanical bit release, assorted subs, bit, and core barrel were lost in the hole. We departed Site U1358 at 1530 h on 7 February because the weather was forecast to significantly deteriorate and we did not want to remain in an area with such high concentrations of ice during the storm. We departed for a deeper water site, Site U1359, where the concentration of icebergs was likely to be very low. Total time on Site U1358 was 22.00 h.

Attempt to return to Site U1358

Later in the expedition and after failed attempts to return to Site U1360, we decided to try to return to Site U1358. During 19 February, we sailed around the western edge of the growing ice field, turned east, and returned to reassess the ice conditions at Site U1358. When we found access to Site U1358 still blocked by ice, we diverted to an alternate shelf site (proposed Site WLSHE-12A) north of Site U1358. We were able to come within 3 nmi of this alternate site when we once more were blocked by heavy ice. At 1630 h on 19 February, we turned north and departed for Site U1359.

Lithostratigraphy

Hole U1358A was drilled to a total depth of 2.0 mbsf and Hole U1358B to a total depth of 35.6 mbsf, both using the RCB system. The upper 8.2 m is unconsoli-

dated and moderately to strongly disturbed by drilling (Cores 318-U1358A-1R and 318-U1358B-1R). Below 8.2 mbsf (Cores 318-U1358B-2R through 4R), the sediments are consolidated and only slightly disturbed by drilling. Based on visual core descriptions and smear slide analyses, Holes U1358A and U1358B penetrated diamictons and diamictites (Fig. F3) and are placed within a single lithostratigraphic unit.

Unit description

Unit I

Interval: 318-U1358B-1R-1, 0 cm, through 4R-1, 19 cm
Depth: 0–28.57 mbsf
Age: Pliocene–Pleistocene

Unit I consists of diamicton and diamictite that transitions between clast-rich muddy and clast-rich sandy composition. The uppermost cores from both holes (Cores 318-U1358A-1R and 318-U1358B-1R) consist of unconsolidated light brownish gray massive clast-rich muddy diamicton that is moderately to strongly disturbed by drilling. Diatoms in trace abundances were identified in smear slides of these cores (see Site U1358 smear slides in "Core descriptions"). Cores below 8.2 mbsf (Cores 318-U1358B-2R through 4R) consist of consolidated greenish gray to gray massive to crudely stratified clast-rich sandy and muddy diamictite. A distinct color change from greenish gray to gray was observed between Cores 318-U1358B-2R and 3R. Below interval 318-U1358B-3R-3, 15 cm (20.45 mbsf), the diamictite is sparsely stratified, with few planar but horizontal to inclined laminations. Clast abundance was visually estimated at between 5% and 7.5%, and clasts are as large as 24 cm. Clast lithologies are variable and include basalt, granitic gneiss, quartzite, and fine-grained metasediments. Clasts have subangular to subrounded shapes and basalt and metasedimentary clasts are often faceted and occasionally striated and fluted.

Interpretation

The diamictons in the upper 8.2 mbsf were probably deposited from floating ice. The diamictites below 8.2 mbsf were either deposited from floating ice (where crudely stratified and laminated) or subglacially, with possible remobilization through glacigenic debris flow.

Clay-mineral X-ray diffraction analysis was performed on only one sample (318-U1358B-3R-1, 10–11 cm), which may not be representative for the entire unit. This sample is derived from a clast-rich sandy diamictite facies, and the clay mineral assemblage is dominated by illite (~80%) and chlorite (~15%). A minor component of smectite (~5%) and a trace amount of kaolinite (<1%) are also present in the sample. The predominance of illite and chlorite is indicative of active physical weathering of granitoid and metamorphic parent rocks in a glacial regime. Similar clay mineral assemblages are typical of Pliocene–Pleistocene sediments of the Wilkes Land margin (e.g., Damiani et al., 2006).

Biostratigraphy

Sediments from Holes U1358A and U1358B contain siliceous and organic microfossils. Calcareous nannofossils and foraminifers were not encountered at Site U1358. Diatoms provide tentative age control throughout the section. Pliocene sediments (between Samples 318-U1358B-2R-CC and 4R-CC; 9.32–28.62 mbsf) are overlain by uppermost Pleistocene to Holocene sediments (Sample 318-U1358A-1R-CC, 1.10 mbsf; and between Samples 318-U1358B-1R-1, 0 cm, and 1R-CC; 0–1.10 mbsf). Dinocysts and radiolarians were encountered in trace amounts only and provide no further age constraints. Diatom assemblages are a mix of sea ice–associated and open-water taxa. This suggests a high-nutrient environmental setting influenced by seasonal sea ice. High abundances of reworked Mesozoic and/or Paleozoic sporomorphs indicate sediment input from the hinterland.

Siliceous microfossils

Samples 318-U1358A-1R-CC (1.10 mbsf) and 318-U1358B-1R-1, 0 cm (0 mbsf), and 1R-CC (0.42 mbsf) contain poor to well-preserved common to abundant diatoms. The diamict matrix of Cores 318-U1358B-2R through 4R (9.32–28.62 mbsf) (see "Lithostratigraphy") contains trace to rare occurrences of diatoms (Table T2), radiolarians, actiniscidians, silicoflagellates, and sponge spicules.

Diatoms

One sample from Hole U1358A and seven samples from Hole U1358B were analyzed for diatoms (Table T2). A characteristic Neogene, high-nutrient, seasonally sea ice–influenced Southern Ocean diatom flora was encountered in all samples. In terms of valve fragmentation, preservation is moderate to poor in Samples 318-U1358A-1R-CC (1.10 mbsf) and 318-U1358B-1R-1, 0 cm (0 mbsf), and poor in all other samples (0.42–28.62 mbsf). In terms of dissolution, diatom preservation is good in all samples analyzed (Table T2).

Samples 318-U1358A-1R-CC (1.10 mbsf) and 318-U1358B-1R-1, 0 cm (0 mbsf), and 1R-CC (0.42 mbsf) contain common to abundant latest Pleistocene to Holocene diatoms characterized by rare to common

occurrences of *Chaetoceros* resting spores, *Eucampia antarctica, Fragilariopsis curta, Fragilariopsis kerguelensis, Fragilariopsis rhombica, Fragilariopsis ritscheri, Fragilariopsis separanda, Shionodiscus gracilis* var. *gracilis, Thalassiosira antarctica,* and *Thalassiosira lentiginosa* (Table T2). We assign these samples to the latest Pleistocene (<0.61 Ma) based on the presence of the index species *T. antarctica* (first occurrence [FO] 0.61 Ma) in association with other latest Pleistocene to Holocene index taxa (Table T3). The absence of *Actinocyclus ingens* (last occurrence [LO] at 0.54 Ma) may further constrain these samples to within the last ~540 k.y.

Samples 318-U1358B-2R-CC through 3R-CC (9.32–21.54 mbsf) contain trace to rare abundances of the Pliocene index taxa *Thalassiosira insigna* and *Thalassiosira inura,* the Miocene–Pleistocene index species *Thalassiosira torokina,* and the long-ranging middle Miocene to late Pleistocene index species *A. ingens* vars. (Tables T2, T3). We tentatively assign these samples to the mid-Pliocene based on the presence of these species and the absence of Pleistocene index taxa listed above. These data imply a mid-Pliocene to latest Pleistocene hiatus or condensed interval between Samples 318-U1358B-1R-CC and 2R-CC (Table T3). Such a hiatus concurs with physical property data, which show changes in magnetic susceptibility and color in the middle of Section 318-U1358B-2R-2 (see **"Physical properties"**). The FO of *T. insigna* (3.25 Ma) and LO of *T. inura* (2.54 Ma) within Samples 318-U1358B-2R-CC and 3R-CC constrain the age of these samples to 3.25–2.54 Ma. The FO of *T. inura* (4.74 Ma) and *T. torokina* (7.23 Ma) and the absence of *T. lentiginosa* (FO at 3.99 Ma) and *F. curta* (FO at 3.56 Ma) indicate an older age for Core 318-U1358B-4R (Table T3). However, because diatoms below Core 318-U1358-2R are heavily fragmented and are in trace to rare abundance, further refinement of the biostratigraphy is difficult. Trace occurrences of radiolarians indicate an age younger than Miocene and therefore do not provide any further insight.

Palynology

One sample (318-U1358B-3R-CC; 21.54 mbsf) was processed for palynology at Site U1358. The sample yielded trace abundances of cysts of heterotrophic dinoflagellates (*Protoperidinium* spp.) in moderate preservation. These dinocysts provide no age constraints. Palynological data are provided in Table T4.

Sporomorphs are abundant in Sample 318-U1358B-3R-CC, and the assemblage mainly consists of well-preserved (saccate) pollen and spores. The dominance of thick-walled and/or chemically particularly resistant taxa (as indicated by the strong representation of spores and bisaccates), the high degree of thermal maturity (as indicated by the dark exine colors), and the lack of *Nothofagus* pollen suggests that the sporomorphs in Sample 318-U1358B-3R-CC are reworked from Mesozoic and/or Paleozoic strata.

Other palynofacies components (i.e., black and brown phytoclasts) are present in trace amounts only.

Age model and sedimentation rates

The spliced succession is divided into two intervals: the uppermost 1.10 m (Samples 318-U1358A-1R-CC and 318-U1358B-1R-1, 0 cm, and 1R-CC) is assigned to the latest Pleistocene to Holocene (<0.54/0.61 Ma) based on diatom biostratigraphy, whereas sediments below this level are no younger than mid-Pliocene (>2.54 Ma) and no older than Miocene. A condensed interval or a hiatus is inferred between Samples 318-U1358B-1R-CC and 2R-CC (0.42 and 9.32 mbsf, respectively), between ~2.54 and 0.54/0.61 Ma. Sedimentation rates are not calculated because our age assignments are largely tentative.

Paleoenvironmental interpretation

Diatom assemblages are a mix of sea ice–associated and open-water taxa. This suggests a high-nutrient environmental setting influenced by seasonal sea ice. Palynological associations are a mix of reworked and in situ palynomorphs. The in situ protoperidinioid dinocysts confirm a nutrient-rich environment. High abundance of reworked microfossils indicates a significant input from the hinterland.

Geochemistry

Organic geochemistry

Gas analysis was performed on three cores in Hole U1358B using the methods described in **"Geochemistry and microbiology"** in the "Methods" chapter. Methane concentrations in the three cores were statistically insignificant (≤2 ppmv).

Inorganic geochemistry

Three sediment samples in Hole U1358B were taken for analyses of percent carbonate and major and trace element analyses (silicon, titanium, aluminum, iron, calcium, magnesium, sodium, potassium, phosphorus, strontium, barium, vanadium, scandium, and cobalt). Data are reported in Table T5.

Physical properties

The physical properties program at Site U1358 included routine runs on the Whole-Round Multisensor Logger (WRMSL), which includes GRA bulk

density, magnetic susceptibility, and *P*-wave logger (PWL) sensors and natural gamma radiation (NGR) measurements. *P*-wave velocity was also analyzed on split cores as well as samples taken for moisture and density (MAD) and porosity analyses.

Whole-Round Multisensor Logger measurements

Magnetic susceptibility

Whole-core magnetic susceptibility was measured at 2.5 cm intervals (2 s measurement time). The raw data values range from 3 to 2834 SI (Fig. F4). However, the majority of measurements vary between 200 and 400 instrument units, with some peaks in Core 318-U1358B-4R representing gravel clasts.

Natural gamma radiation

NGR counts range from 33 to 99 cps, with higher values in the two deeper cores in Hole U1358B. Cores 318-U1358B-3R and 4R show variability on the order of ~50–60 cm, possibly reflecting the alternations of muddy versus sandy diamictites (Fig. F4).

Gamma ray attenuation bulk density

GRA density was measured at 2.5 cm intervals on the WRMSL (using a 10 s integration time). Variations in GRA density reflect variations in the composition of the Pliocene–Pleistocene diamictite that varies between clast-rich muddy and clast-rich sandy lithologies. The GRA density values for the consolidated sediments are as dense as 2.7 g/cm^3 (Fig. F5).

P-wave velocity

P-wave velocity measurements were made at 5 cm intervals on the PWL on the WRMSL for Hole U1358B. These measurements range from 1571 to 2867 m/s (Fig. F6). Additionally, split core *P*-wave velocity measurements were taken using the Section Half Velocity Gantry. These measurements were made once per section and range from 1414 to 6137 m/s. In general, the *P*-wave measurements on the split cores should be considered more reliable since the reduced diameter of the RCB cores negatively impacted the WRMSL data (Fig. F6).

Moisture and density measurements

Measurements of density, porosity, and grain density were made on seven samples of cores from Hole U1358B. Dependent on core recovery and quality, one sample was taken per section. These samples were measured for wet mass, dry mass, and dry volume and, using these measurements, porosity, percent water mass, and dry density. Bulk density and grain density were also calculated. The bulk densities (MAD) from discrete samples range from 2.1 to 2.46 g/cm^3 (Fig. F5). In the upper two cores of the hole, both the GRA densities and the wet bulk densities on samples (MAD) correlate well. However, from Core 318-U1358B-3R downhole, the GRA density results are consistently lower than those measured from physical samples. We interpret this to be a result of the reduced diameter of the RCB cores. This reduced diameter, especially pronounced in the diamictites recovered at this site, likely systematically underestimated the bulk density as measured by the GRA densiometer (Fig. F5).

The porosity ranges from 35% to 25% (Fig. F7) and overall decreases with depth. Grain densities range from 2.59 to 3.10 g/cm^3. These values are slightly higher than expected for the recovered sediment type and are most likely related to the clast abundance and their variable compositions that include basalt, granitic gneiss, quartzite, fine-grained metasediments, and especially the occurrence of pyrite throughout the sediment (up to 4%; see **"Lithostratigraphy"**).

References

Cooper, A.K., Brancolini, G., Escutia, C., Kristoffersen, Y., Larter, R., Leitchenkov, G., O'Brien P., and Jokat, W., 2009. Cenozoic climate history from seismic reflection and drilling studies on the Antarctic continental margin. *In* Florindo, F., and Siegert, M. (Eds.), *Developments in Earth and Environmental Sciences* (Vol. 8): *Antarctic Climate Evolution:* Amsterdam (Elsevier), 115–228.

Damiani, D., Giorgetti, G., and Memmi Turbanti, I., 2006. Clay mineral fluctuations and surface textural analysis of quartz grains in Pliocene–Quaternary marine sediments from Wilkes Land continental rise (East Antarctica): paleoenvironmental significance. *Mar. Geol.,* 226(3–4):281–295. **doi:10.1016/j.margeo.2005.11.002**

De Santis, L., Brancolini, G., and Donda, F., 2003. Seismostratigraphic analysis of the Wilkes Land Continental Margin (East Antarctica): influence of glacially driven processes on the Cenozoic deposition. *Deep-Sea Res., Part II,* 50(8–9):1563–1594. **doi:10.1016/S0967-0645(03)00079-1**

Eittreim, S.L., Cooper, A.K., and Wannesson, J., 1995. Seismic stratigraphic evidence of ice-sheet advances on the Wilkes Land margin of Antarctica. *Sediment. Geol.,* 96(1–2):131–156. **doi:10.1016/0037-0738(94)00130-M**

Escutia C., De Santis, L., Donda, F., Dunbar, R.B., Cooper, A.K., Brancolini, G., and Eittreim, S.L., 2005. Cenozoic ice sheet history from East Antarctic Wilkes Land Continental Margin sediments. *Global Planet. Change,* 45(1–3):51–81. **doi:10.1016/j.gloplacha.2004.09.010**

Escutia, C., Eittreim, S.L., and Cooper, A.K., 1997. Cenozoic sedimentation on the Wilkes Land continental rise, Antarctica. *In* Ricci, C.A. (Ed.), *The Antarctic Region: Geo-*

logical Evolution and Processes. Proc. Int. Symp. Antarct. Earth Sci., 7:791–795.

Harwood, D.M., and Maruyama, T., 1992. Middle Eocene to Pleistocene diatom biostratigraphy of Southern Ocean sediments from the Kerguelen Plateau, Leg 120. *In* Wise, S.W., Jr., Schlich, R., et al., *Proc. ODP, Sci. Results,* 120: College Station, TX (Ocean Drilling Program), 683–733. **doi:10.2973/odp.proc.sr.120.160.1992**

O'Brien, P.E., Cooper, A.K., Richter, C., et al., 2001. *Proc. ODP, Init. Repts.,* 188: College Station, TX (Ocean Drilling Program). **doi:10.2973/odp.proc.ir.188.2001**

Passchier, S., O'Brien, P.E., Damuth, J.E., Januszczak, N., Handwerger, D.A., and Whitehead, J.M., 2003. Pliocene–Pleistocene glaciomarine sedimentation in eastern Prydz Bay and development of the Prydz trough-mouth fan, ODP Sites 1166 and 1167, East Antarctica. *Mar. Geol.,*199(3–4):279–305. **doi:10.1016/S0025-3227(03)00160-9**

Rebesco, M., Camerlenghi, A., Geletti, R., and Canals, M., 2006. Margin architecture reveals the transition to the modern Antarctic ice sheet (AIS) ca. 3 Ma. *Geology,* 34(4):301–304. **doi:10.1130/G22000.1**

Publication: 2 July 2011
MS 318-106

Figure F1. Bathymetric map of eastern Wilkes Land continental shelf showing the location of Sites U1357, U1358, and U1360. Bold black line = multichannel seismic reflection Profile IFP 108 shown in Figure F2 and Figure F1 in the "Site U1360" chapter.

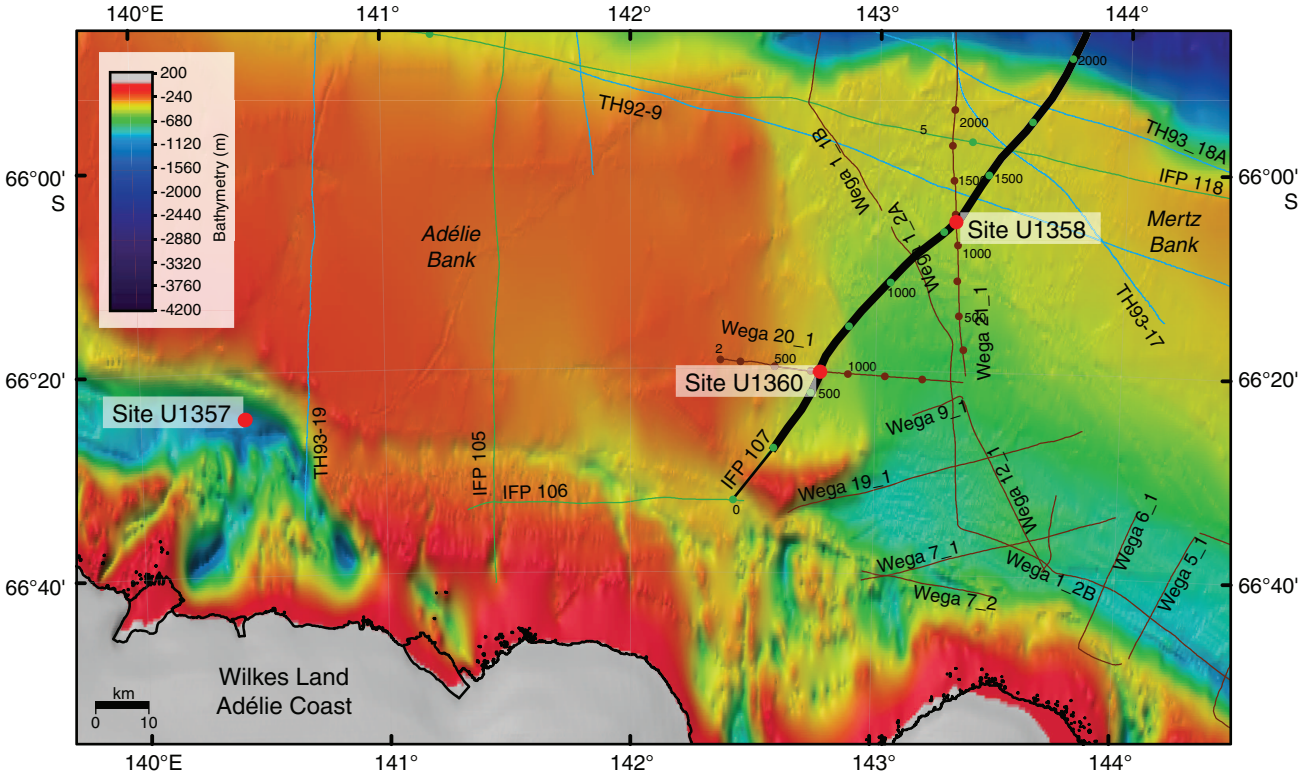

Figure F2. Multichannel seismic reflection Profile IFP 107 across Site U1358. Profile shows main regional unconformities defined in the Wilkes Land continental shelf. Drilling at Site U1358 targeted unconformity WL-U8. Red rectangle = approximate penetration achieved at Site U1358. Location of seismic profile is shown in Figure F1.

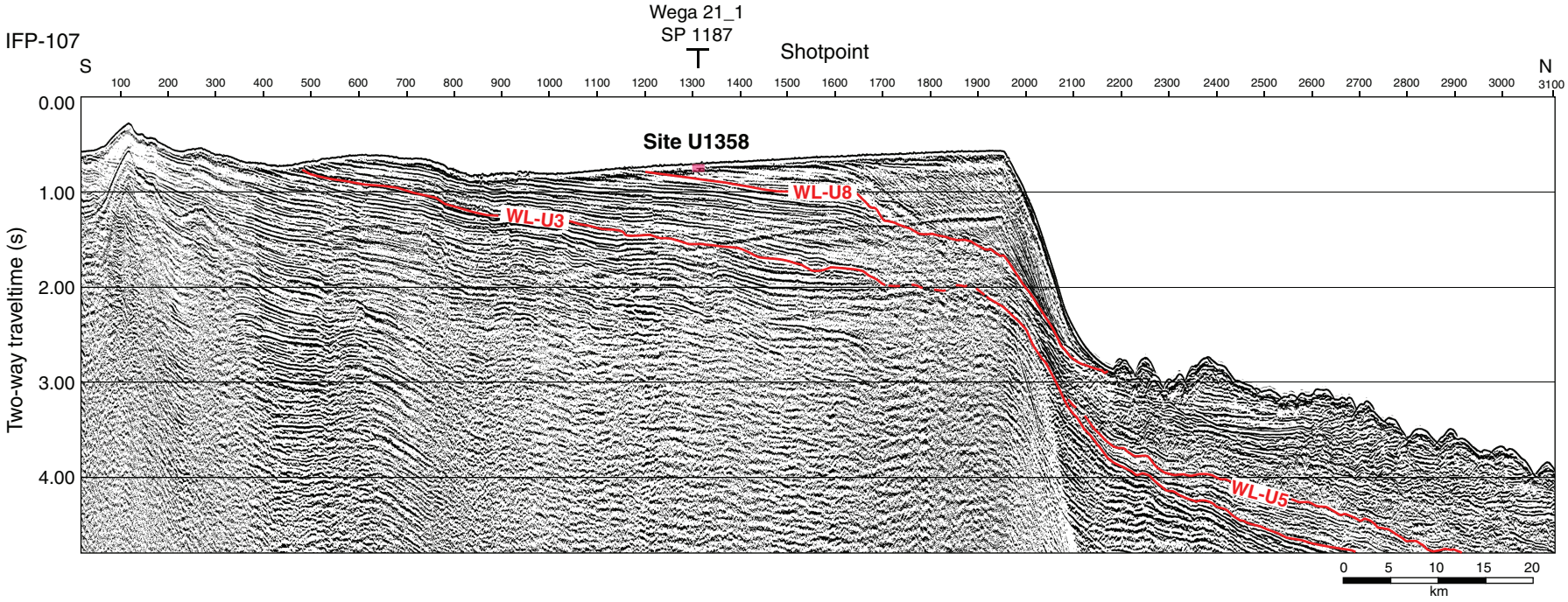

Figure F3. Core image of diamictite, Hole U1358B (interval 318-U1358B-4R-1, 36–72 cm).

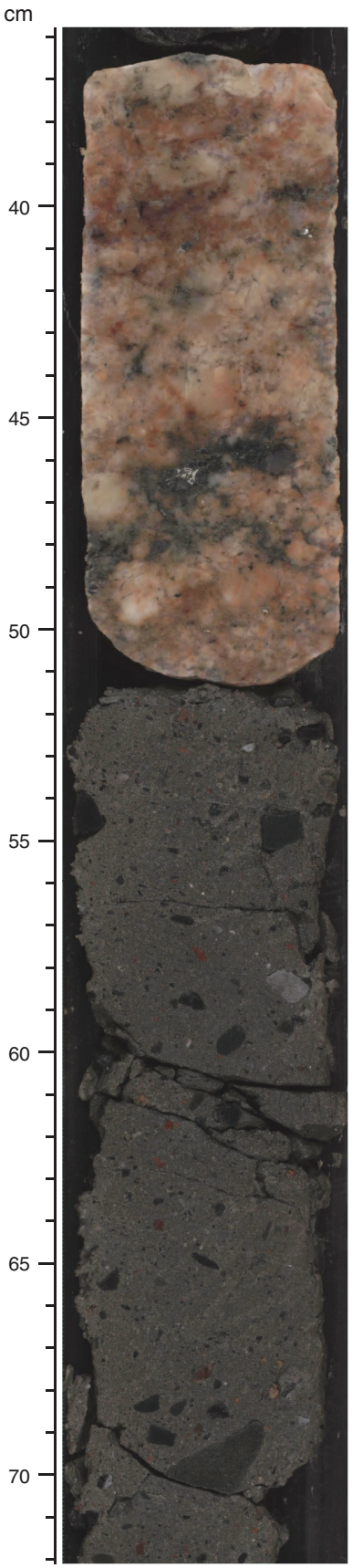

Figure F4. Plots of magnetic susceptibility and natural gamma radiation (NGR) data, Site U1358.

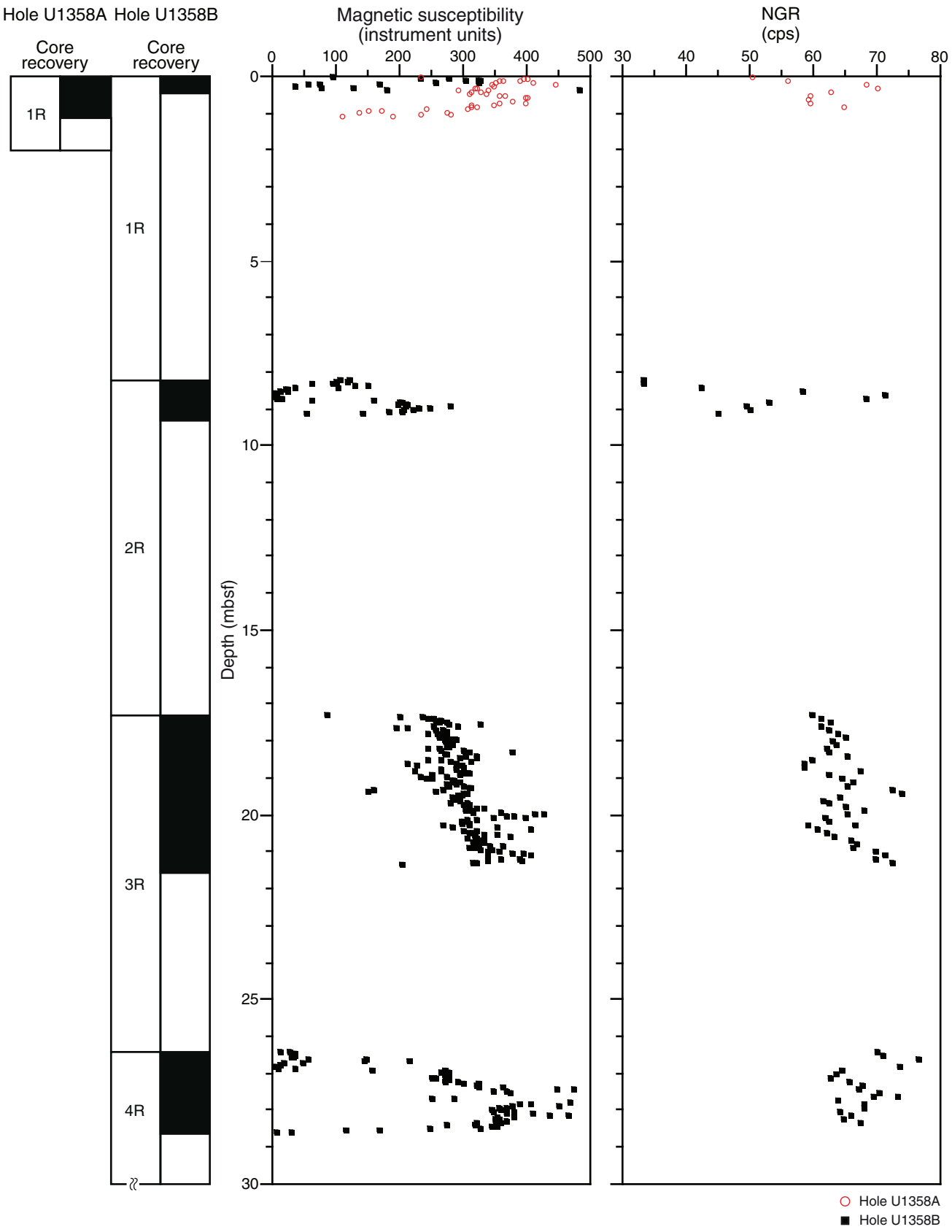

Figure F5. Plot of comparison of gamma ray attenuation (GRA) bulk density data and wet bulk density from moisture and density (MAD) discrete measurements, Site U1358.

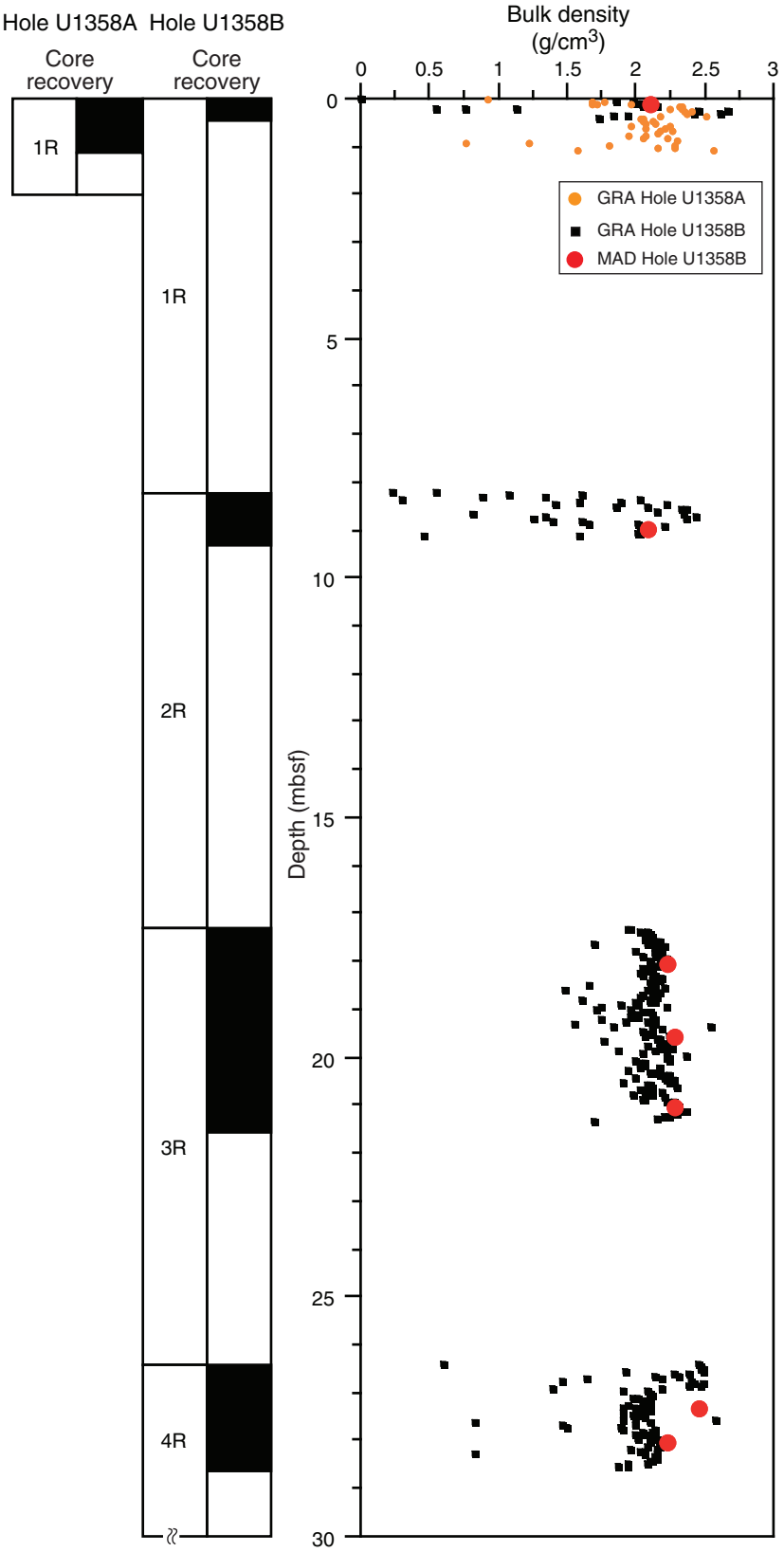

Figure F6. Plot of *P*-wave logger (PWL) and Section Half Velocity Gantry data, Hole U1358B.

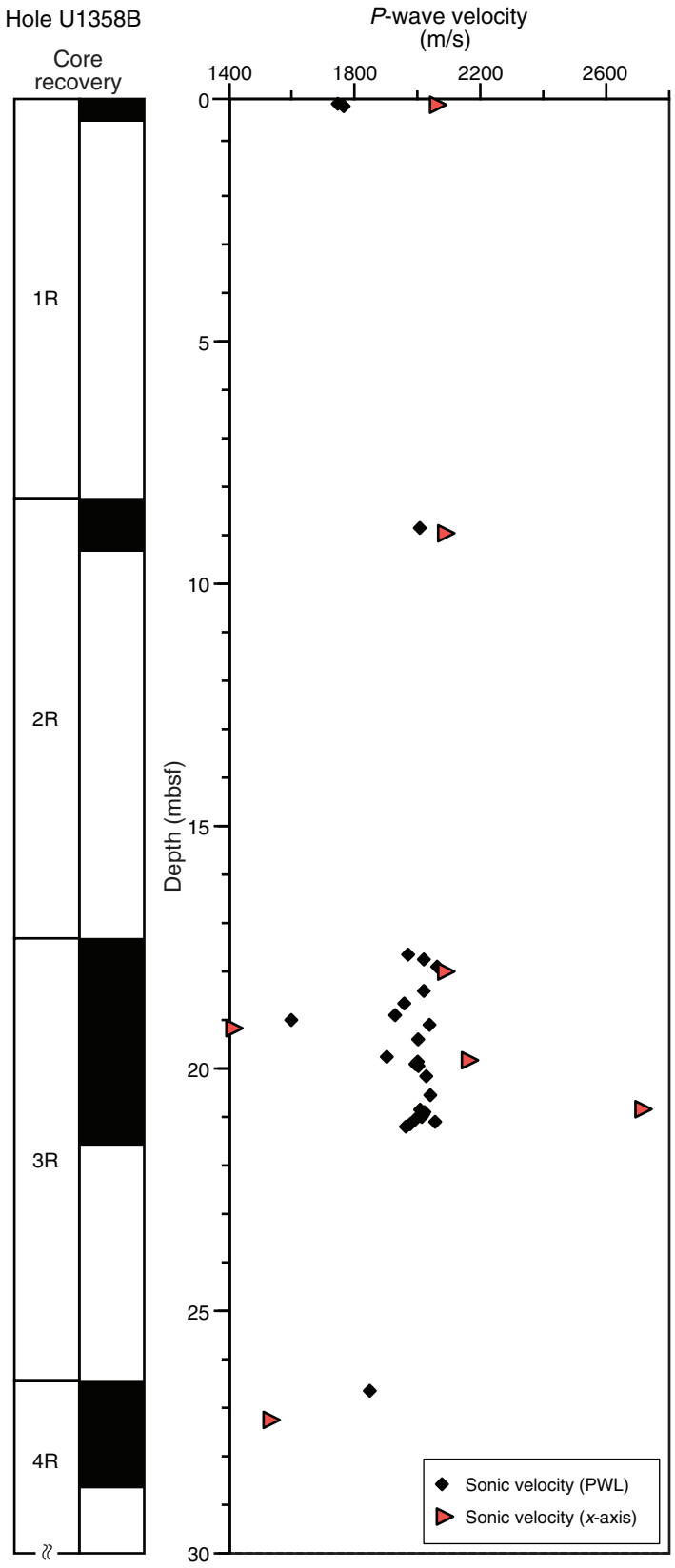

Figure F7. Plots of grain density and porosity from discrete measurements, Site U1358.

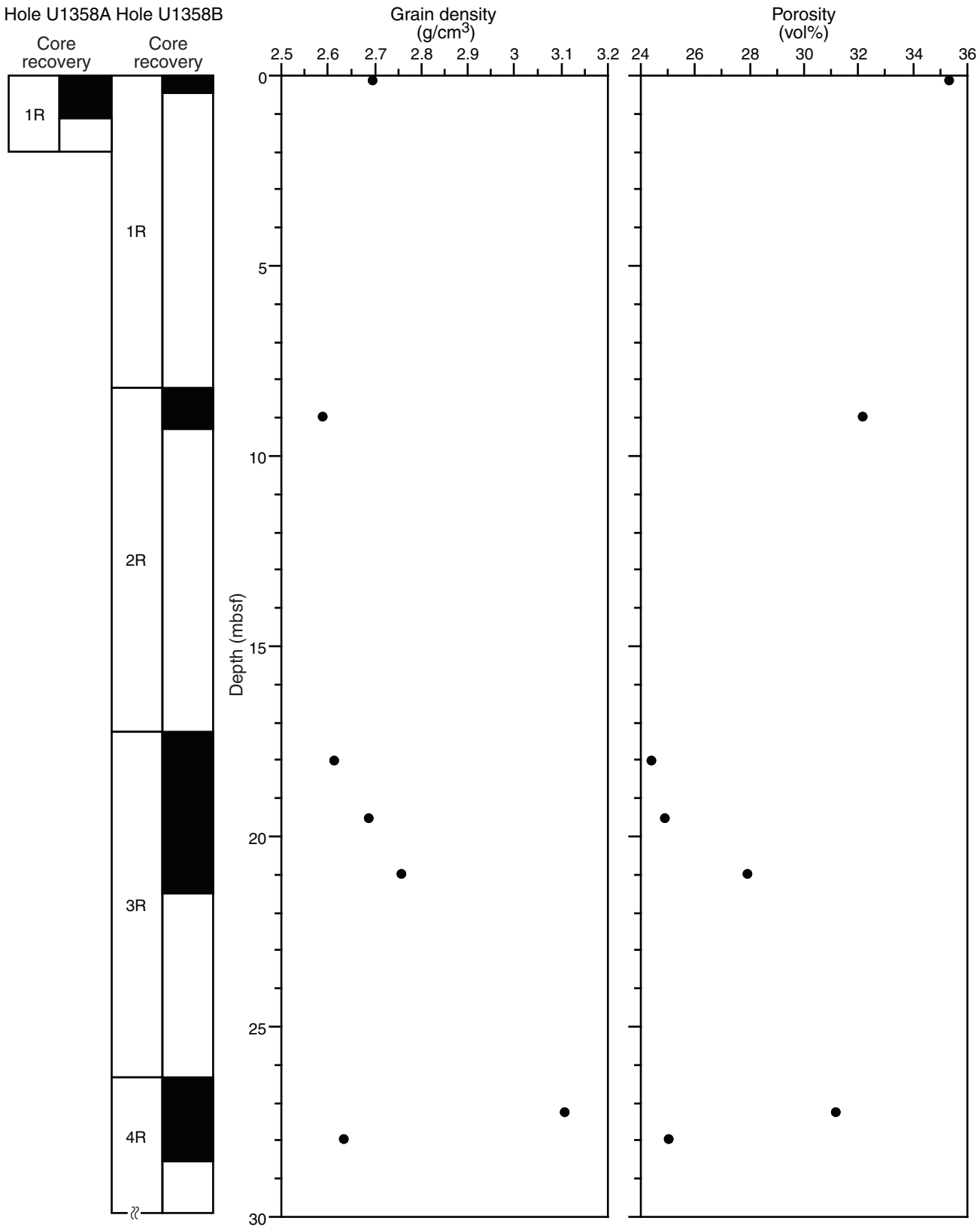

Table T1. Coring summary, Site U1358. (See table notes.)

Site U1358
Time on site (h): 22.00 (1730 h, 6 February–1530 h, 7 February 2010)

Hole U1358A
Latitude: 66°05.4247′S
Longitude: 143°18.7674′E
Time on hole (h): 6.75 (1730 h, 6 February–0015 h, 7 February 2010)
Seafloor (drill pipe measurement from rig floor, m DRF): 510.0
Distance between rig floor and sea level (m): 11.0
Water depth (drill pipe measurement from sea level, m): 499.0
Total penetration (m DSF): 2.0
Total depth (drill pipe measurement from rig floor, m DRF): 501.0
Total length of cored section (m): 2.00
Total core recovered (m): 1.10
Core recovery (%): 55
Total number of cores: 1

Hole U1358B
Latitude: 66°05.4244′S
Longitude: 143°18.7666′E
Time on hole (h): 15.25 (0015 h, 7 February–1530 h, 7 February 2010)
Seafloor (drill pipe measurement from rig floor, m DRF): 510.0
Distance between rig floor and sea level (m): 11.0
Water depth (drill pipe measurement from sea level, m): 499.0
Total penetration (m DSF): 35.6
Total depth (drill pipe measurement from rig floor, m DRF): 534.6
Total length of cored section (m): 35.6
Total core recovered (m): 8.00
Core recovery (%): 22
Total number of cores: 4

			Depth DSF-A (m)			Depth CSF-A (m)			
Core	Date (2010)	Local time (h)	Top of cored interval	Bottom of cored interval	Interval advanced (m)	Top of cored interval	Bottom of cored interval	Length of core recovered (m)	Recovery (%)
318-U1358A-									
1R	7 Feb	0055	0.0	2.0	2.0	0.0	1.10	1.10	55
				Cored totals:	2.0			1.10	55
				Total interval cored:	2.0				
318-U1358B-									
1R	7 Feb	0430	0.0	8.2	8.2	0.0	0.42	0.42	5
2R	7 Feb	0610	8.2	17.3	9.1	8.2	9.32	1.12	12
3R	7 Feb	0810	17.3	26.4	9.1	17.3	21.54	4.24	47
4R	7 Feb	0935	26.4	35.6	9.2	26.4	28.62	2.22	24
				Cored totals:	35.6			8.00	22
				Total interval cored:	35.6				

Notes: DRF = drilling depth below rig floor. DSF-A = drilling depth below seafloor determined by tagging seafloor, CSF-A = core depth below seafloor, overlap if long. Local time = UTC + 11 h.

Table T2. Siliceous microfossil abundance and preservation, Hole U1358A. (**See table notes.**)

Core, section, interval (cm)	Depth (mbsf)		Abundance	Preservation	Diatoms																																																						
	Top	Bottom			Preservation - dissolution	*Actinocyclus actinochilus*	*Actinocyclus ingens* var. *ingens*	*Actinocyclus ingens* var. *ovalis*	*Actinocyclus* sp. cf. *A. actinochilus*	*Actinocyclus* spp.	*Asteromphalus parvulus*	*Azpeitia tabularis*	*Chaetoceros* spp. (resting spores)	*Cocconeis* spp.	*Coscinodiscus asteromphalus*	*Coscinodiscus* spp.	*Dactyliosolen antarcticus*	*Denticulopsis delicata*	*Denticulopsis* aff. *seminae*	*Denticulopsis simonsenii*	*Denticulopsis* spp.	*Eucampia antarctica*	*Eustephanias* spp.	*Fragilariopsis curta*	*Fragilariopsis kerguelensis*	*Fragilariopsis obliquecostata*	*Fragilariopsis rhombica*	*Fragilariopsis ritscheri*	*Fragilariopsis separanda*	*Fragilariopsis* spp.	*Paralia sulcata*	*Paralia sulcata* var. *crenulata*	*Porosira glacialis*	*Rhizosolenia* spp.	*Rouxia* spp.	*Shionodiscus gracilis* var. *expectus*	*Shionodiscus gracilis* var. *gracilis*	*Shionodiscus oestrupii*	*Stellarima microtrias*	*Stephanopyxis* spp.	*Thalassionema nitzschioides*	*Thalassiosira antarctica*	*Thalassiosira insigna*	*Thalassiosira inura*	*Thalassiosira lentiginosa*	*Thalassiosira oliverana*	*Thalassiosira poroseriata*	*Thalassiosira* sp. A of Harwood, 1986	*Thalassiosira* spp.	*Thalassiosira torokina*	*Thalassiosira vulnifica*	*Thalassiothrix antarctica*	*Thalassiothrix longissima*	*Trichotoxon reinboldii*	*Trinacria* sp.	*Vallodiscus* sp.	Actiniscidians	Silicoflagellates	Sponge spicules
318-U1358A-																																																											
1R-CC	0.90	1.10	C	P–M	G	X						X	C				X					X		C	C	X	C		R	X			X	X			F		X			F			F				X				X	X			R		
318-U1358B-																																																											
1R-1, 0	0.00	0.00	A	M	G	X			X		X			X			X					F		F	C		F	R	X					X		R	R	X	X			R			R	X	X		X									X	
1R-CC	0.23	0.42	C	P	G	X						X	C	X			X	X				F		F	C	X	C	X	F	X			X	X			C					F			X				X		?	X	R						
2R-CC	9.13	9.32	R	P	G								X								X	X									X			X					X				X	R						X		X							X
3R-2, 24–25	19.03	19.04	X	P	G		X			X			X		X	X							X											X	X			X			X			X		X				X		X		X					
3R-CC	21.34	21.54	X	P	G									X			X	X	X		X													X	X		X						X	X		X				X		X	X						
4R-1, 92	27.32	27.32	X	P	G																X													X					X	X	X			X				X							X	X			
4R-CC	28.38	28.62	X	P	G			X											X	X																		X	X	X										X			X						

Notes: * = early form, see Harwood and Maruyama (1992). Data excludes radiolarians. Abundance: A = abundant, C = common, R = rare, X = trace. Preservation: G = good, M= medium, P = poor, ? = uncertainty. See **"Biostratigraphy"** in the "Methods" chapter for abundance and preservation definitions.

Table T3. Diatom biostratigraphic datums, Site U1358. (See table note.)

Event	Published age (Ma)	Error (m.y.)	Core, section, interval (cm) Top	Core, section, interval (cm) Bottom	Depth (mbsf) Top	Depth (mbsf) Bottom
			318-U1358A-	318-U1358A-		
FO *Thalassiosira antarctica*	0.61	0.04		1R-CC		1.10
FO *Fragilariopsis rhombica*	1.41	0.04		1R-CC		1.10
FO *Fragilariopsis separanda*	1.41	0.04		1R-CC		1.10
FO *Shionodiscus gracilis* var. *gracilis*	1.87	0.00		1R-CC		1.10
FO *Fragilariopsis kerguelensis*	2.29	0.01		1R-CC		1.10
FO *Actinocyclus actinochilus*	2.77	0.04		1R-CC		1.10
FO *Fragilariopsis ritscheri*	2.85	0.03		1R-CC		1.10
FO *Fragilariopsis curta*	3.56	0.01		1R-CC		1.10
FO *Thalassiosira lentiginosa*	3.99	0.13		1R-CC		1.10
			318-U1358B-	318-U1358B-		
FO *Thalassiosira antarctica*	0.61	0.04	1R-1, 0	1R-CC	0.00	0.42
FO *Fragilariopsis rhombica*	1.41	0.04	1R-1, 0	1R-CC	0.00	0.42
FO *Fragilariopsis separanda*	1.41	0.04	1R-1, 0	1R-CC	0.00	0.42
FO *Shionodiscus gracilis* var. *gracilis*	1.87	0.00	1R-1, 0	1R-CC	0.00	0.42
FO *Fragilariopsis kerguelensis*	2.29	0.01	1R-1, 0	1R-CC	0.00	0.42
FO *Actinocyclus actinochilus*	2.77	0.04	1R-1, 0	1R-CC	0.00	0.42
FO *Fragilariopsis ritscheri*	2.85	0.03	1R-1, 0	1R-CC	0.00	0.42
FO *Fragilariopsis curta*	3.56	0.01	1R-1, 0	1R-CC	0.00	0.42
FO *Thalassiosira lentiginosa*	3.99	0.13	1R-1, 0	1R-CC	0.00	0.42
LO *Thalassiosira torokina*	2.24	0.04	1R-CC	2R-CC	0.42	9.32
LO *Thalassiosira insigna*	2.48	0.03	1R-CC	2R-CC	0.42	9.32
LO *Thalassiosira inura*	2.54	0.01	1R-CC	2R-CC	0.42	9.32
FO *Thalassiosira insigna*	3.25	0.11	3R-CC	4R-1, 92	21.54	27.32
FO *Thalassiosira inura*	4.74	0.03	4R-1, 92	4R-CC	27.32	28.62
FO *Thalassiosira torokina*	7.23	0.80	4R-CC	4R-CC	28.62	28.62

Note: FO = first occurrence, LO = last occurrence.

Table T4. Palynology, Hole U1358B. (See table notes.)

Core, section, interval (cm)	Depth (mbsf) Top	Depth (mbsf) Bottom	Abundance	Preservation	Dinocysts	Sporomorphs	Acritarchs	Foraminifer test linings	Black phytoclasts	Brown phytoclasts	Amorphous organic matter	Saccate pollen	*Nothofagus* pollen	Other pollen	Spores	Fungal spores	Reworked sporomorphs	*Brigantedinium* spp.
318-U1358B- 3R-CC, 6	21.4	21.4	A	M	T	A	B	B	B	F	B	C	B	F	A	B	30	2

Notes: Abundance: A = abundant, C = common, F = few, T = trace, B = barren. Preservation: M = medium. See "Biostratigraphy" in the "Methods" chapter for abundance and preservation definitions.

Table T5. Major and trace element concentrations, Site U1358. (See table notes.)

Core, section, interval (cm)	Depth (mbsf)	Major element oxide (wt%) SiO_2	TiO_2	Al_2O_3	Fe_2O_3	MgO	CaO	Na_2O	K_2O	P_2O_5	Trace element (ppm) Ba	Sr	V	Sc	Co	$CaCO_3$ (wt%)
318-U1358B-																
1R-1, 10–11	0.11	71.93	0.54	12.36	4.40	2.27	2.98	2.47	2.81	0.15	547	181	61	10	36	2.8
3R-1, 10–11	17.40	72.46	0.53	12.37	4.30	2.14	2.68	2.38	2.89	0.16	598	178	59	9	26	2.6
4R-1, 86–87	27.26	70.56	0.57	13.06	4.55	2.36	2.93	2.47	3.25	0.15	657	185	64	9	29	3.4

Notes: Major element oxides normalized to 100 wt%. Typical errors are 1%–5% for all elements over the course of two ICP-AES runs during which the samples were analyzed. $CaCO_3$ contents were determined by coulometer.